Research Article

Modeling and Simulation of a Gas Discharge LENR Prototype

Bob Higgins[*] and   Dennis G. Letts

Industrial Heat, 310 S. West Street, Raleigh, NC 27603, USA

Abstract

Modeling of a thermal system is described using circuit analogues and the highly developed SPICE simulator operating in nonlinear transient mode. Thermal circuit modeling is shown to provide a good fit in a Seebeck calorimeter, even for complex experimental thermal behavior. Component values are either derived or extracted for the calorimeter. The resulting model is used to correct for experimental measurement deficiencies, and to deconvolve the excess heat (XH) waveform (residual) from the output response. Model computation time is less than 5 s for typical circuits on an average contemporary personal computer. Also, during the course of modeling the calorimeter, experimental evidence was found for the obscure phenomenon of nonFourier heat transfer.
ⓒ 2019 ISCMNS. All rights reserved. ISSN   2227-3123

Keywords: Deconvolution, Non-Fourier heat propagation, SPICE, Thermal modeling

1. Introduction

There are several options to model thermal systems – from the most fundamental formulations as finite element discretizations to simplified analytic parameter fits. Finite element analysis is the most complex to setup, and for the Letts calorimeter, modeling could take years of development and simulation to achieve a satisfactory result. On the other end of the spectrum, analytic parameter fits provide little correspondence to the physical attributes of the system, provide little understanding of the cause for behavior, and limitations to the applicability of the fit are not always apparent.

Between these two extremes lies thermal circuit modeling. This technique uses simple electrical circuit analogues for fundamental heat sources, temperature sinks, thermal flow resistance, and thermal storage. System models are constructed with connections of these components having direct correspondence to the physical system. The resulting thermal "circuit model" can represent the complete dynamic thermal response of the system to an experimental heat waveform input. Agreement between experiment and simulated data can be remarkable. The response can be computed in less than 1 s using a modern personal computer.

The preferred simulator for such modeling is SPICE[a]. The SPICE simulator is a nonlinear circuit simulator available for free from several vendors with an excellent graphical user interface. The SPICE based simulator used for

---

[*]Corresponding author. E-mail: bhiggins@industrialheat.co.
[a]SPICE – Simulation Program with Integrated Circuit Emphasis. A common core electrical engineering simulation tool based upon numerical integration, and capable of handling nonlinear circuits in transient simulation mode.

this project was SIMetrix/SIMPLIS^TM Elements (hereafter referred to simply as SIMetrix). It is a free version of their commercial simulation environment having full functionality but limited number of simulation nodes. This limitation in maximum nodes is unlikely to impact most thermal modeling problems. The SIMetrix modeling suite [1] has many desirable features including support for variables (for computed component values), non-linear elements, and the capability to drive the model sources from experimental data.

First, the basics of thermal circuit modeling are described. This is followed by application of thermal circuit simulation (using SIMetrix) to model the Letts gas discharge reactor system and its surrounding calorimeter.

2. Thermal Modeling with Electrical Circuit Analogues

Only a small subset of the SPICE supported model elements are required for ordinary thermal modeling. The fundamental components are as follows.

- *Thermal resistance* – resistance to heat flow across a temperature difference.
- *Thermal capacity* – heat storage; fundamental in dynamic thermal modeling.
- *Heat source* – this could be any source of heat, including electrical dissipation.
- *Temperature sink* – a place in the circuit where the temperature is known or fixed.

The following sections describe each of these and how they correspond to their electrical analogues.

2.1. Thermal resistance

The thermal resistance is the simplest and most fundamental thermal modeling component. It represents the heat flow as a function of temperature difference. Figure 1 shows the correspondence between the electrical quantities and the thermal quantities. Understanding this correspondence directly leads one to understand how circuit simulation is used with thermal quantities.

In Fig. 1, the normal resistor's electrical quantities are shown in blue. The definition of the electrical resistance, R_e, via Ohm's law is

$$R_e = \frac{\Delta \text{ voltage across element}}{\text{current through element}} \text{ (V/A)}.$$

A voltage difference across the resistor causes a flow of charge through the resistor and the rate of flow of charge is a current.

In the thermal resistance, heat flows through the resistance depending linearly (normally) upon the temperature difference across the resistive flow path.

$$R_{th} = \frac{\Delta \text{ temperature across element}}{\text{heat in watts}} \text{ (°C/W)}.$$

The correspondence is that heat flow in watts is equivalent to current and temperature corresponds to voltage in the electrical domain. And, with those two analogues ($I \leftrightarrow W$, and $V \leftrightarrow T$), the thermal resistance in °C/W corresponds directly to electrical resistance in ohms.

Thermal resistance is used to model any heat flow. The thermal resistance may be low if the conducting path is through a metal, or it may be a high resistance if the conducting path is through gas.

Thermal resistance may not be a simple constant. In fact, when modeling heat flow to ambient over large temperature ranges, the best model will be a nonlinear resistance (versus temperature) to account for heat flow via convection

$$R_e = \frac{(V_1 - V_2)}{i} = \frac{Volts}{Amp}$$
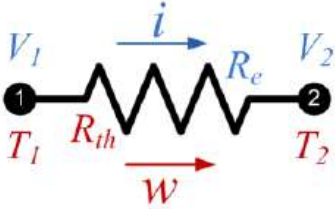
$$R_{th} = \frac{(T_1 - T_2)}{w} = \frac{{}^\circ C}{watt}$$

Figure 1. Thermal resistance correspondence to electrical resistance.

and radiation. By utilizing test experimental data over a wide temperature range, a good fit can be obtained for the nonlinear resistance using a simple low-order polynomial representation of the resistance – even when the temperature range being modeled spans more than $1000^\circ C$.

The electrical analogue equivalence described above suggest that introducing heat into a circuit is done by introducing a current in the electrical circuit – e.g. using a current source. A temperature sink (a place/node where the temperature is known or constant) may be implemented simply as a voltage source (a source that has a forced voltage corresponds to a thermal source that has a forced temperature).

These fundamental correspondences ($I \leftrightarrow W$ and $V \leftrightarrow T$) set the stage for the whole of circuit based thermal simulation.

2.2. Thermal capacity

Thermal capacity is the ability of an object (mass) to store heat. The copper block in the Letts calorimeter has a high thermal capacity – its mass is high. Heat (Q) is commonly measured in joules. Electrical current is the rate of flow of the charge. Heat flow, in joules/second, is equivalent to watts. A mass that stores heat accumulates heat like a capacitor accumulates charge. For an object with a given thermal capacity, the more heat one adds, the higher the temperature of the object.

Interestingly, electrical capacitors are flexibly used in electrical circuits with both terminals free for interconnection in the circuit. However, capacitors in thermal circuit modeling are always connected with one of the leads connected to the reference (ground) node. Thermal capacity is the fundamental element needed to model the dynamics in a thermal system.

Thermal capacity can readily be estimated based upon the material and it's mass. For example, consider the copper block in the calorimeter. Pure copper has a heat capacity of 24.44 J/(mol $^\circ C$). The copper molar mass is also listed as 63.546 g/mol. Thus, the heat capacity is 0.385 J/g $^\circ C$. Knowing the weight of copper in the central calorimeter block, the thermal capacity of the block can be calculated as $C_{th} = 0.385$ (block weight in g) in J/$^\circ C$. How this capacity is used in thermal modeling will be described in subsequent sections.
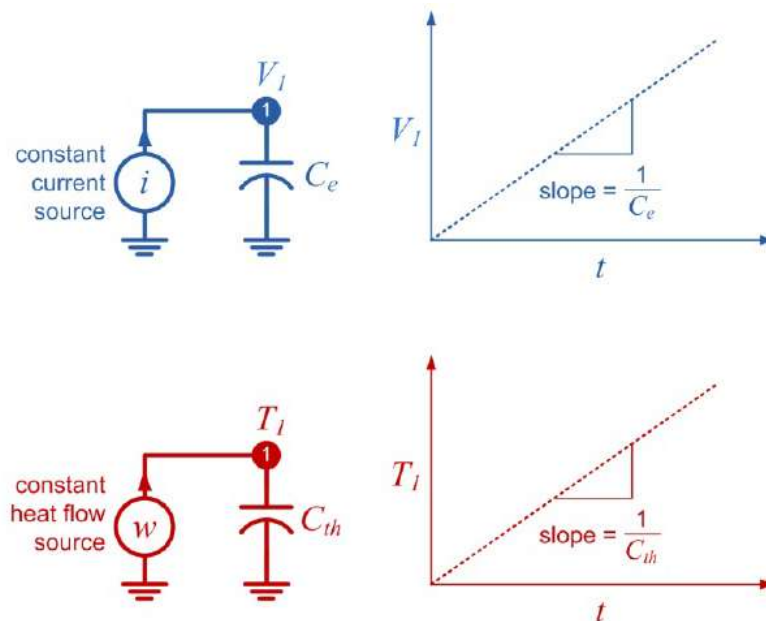
Figure 2.   Thermal capacity correspondence to electrical capacity.

2.3. Heat sources

The thermal model is used to compute the thermal response of the system (at various measurement points) to thermal inputs, primarily heat sources. Heat may come from many places in the system, and regardless of type, it can be modeled as an electrical current source. As Fig. 2 suggests an electrical constant current source models a constant source of heat in watts. However, a current source can also be a time dependent waveform. If an ideal waveform is to be tested, the current source may be configured in the simulator as a current waveform generator.

The SIMetrix SPICE simulator provides a very useful general current waveform generator – one that can be driven from a file. This source is called a PWL source for "Piece-Wise Linear". A file name is supplied for the source – within this text file, samples of (time (in seconds) current (in amps)) are supplied, one sample in each record (see Fig. 3). The simulator interpolates linearly between the supplied samples as it computes the response. Interpolation is required because SPICE does not simulate the response with uniform time steps (and uniform time steps are not required for the PWL data file). The SPICE transient solver varies the time steps automatically as needed to maintain the accuracy of the numerical integration. The utility of the PWL source is that heat input into the experiment is typically recorded as part of the sampled data. This exact experimental input can be extracted as a 2-column text file and used to drive the model with the actual heat input waveform that was used in the experiment. Parameter values (thermal resistance and capacity values, and/or circuit topology) are adjusted such that the simulated output response agrees with measured output response obtained when being driven with the actual experimental input heat waveform.

How heat sources are employed will be described in application to the Letts calorimeter modeling is shown in Table 1.

Table 1. Text data file for driving a PWL source.

|	
0.0	27.95
60.0	27.97
120.0	27.98
180.0	27.97
240.0	28.02
300.0	27.96

2.4. Temperature sinks

In almost all thermal systems there will be certain points in the model where the temperature is either held constant, or it is known. This temperature "sink" may be modeled using an electrical voltage source to ground (the thermal analogue of voltage is temperature). Thus, a voltage source in the model represents a node at known temperature. For example, suppose there was a place in the system that was water cooled and regulated to 28°C. This could be modeled in the electrical circuit as a voltage source to ground with a voltage of 28 V.

For the common case where the temperature of a thermal sink is not constant, but varies with time across the experiment, and presuming its temperature is recorded, a PWL voltage source may be used to force exactly this behavior within the model. The experimentally measured data for the temperature at that modeled location is extracted into a 2-column text file and used to drive the PWL voltage/temperature source during simulation. This useful feature will be frequently incorporated into thermal models.

2.5. Thermoelectric (Seebeck) generator modules

In the Letts calorimeter, heat flow is measured by proxy in the generated output voltage from a set of thermoelectric generator (TEG) modules. Figure 3 shows a sample cross-section of these modules in the Letts calorimeter between the copper block of the calorimeter and the finned aluminum heat sinks.
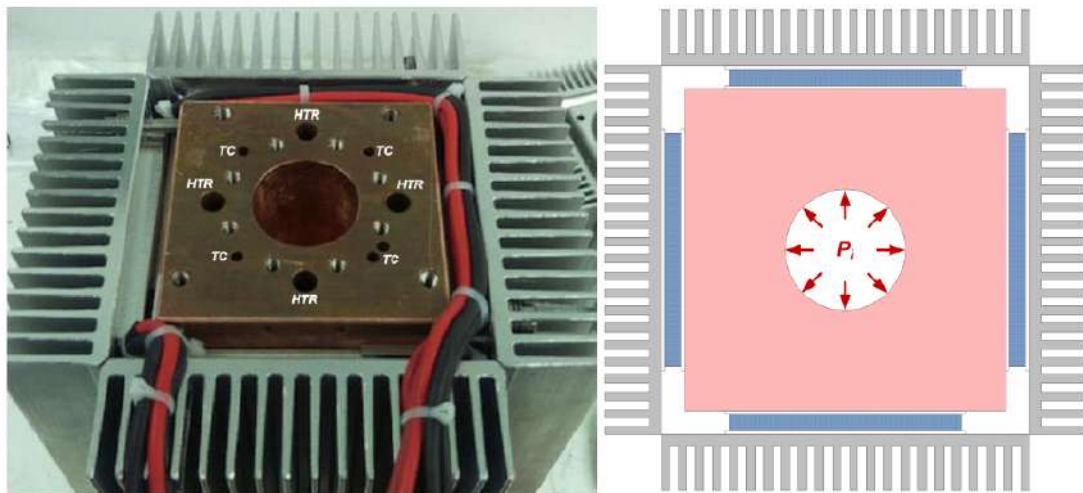
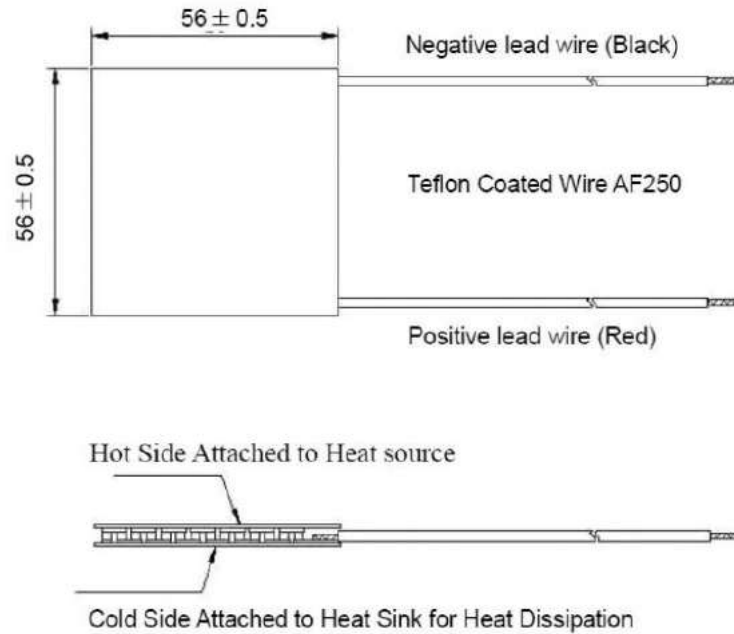**Figure 3.** Letts calorimeter cross-section showing TEG module location.

Figure 4.   TECTEG TEG1-12611-6.0 TEG module drawing.

Figure 4 shows the module dimensions used in the Letts calorimeter. The drawing also shows the modules having thin ceramic (typically alumina) electrically insulating but thermally conductive plates with semiconductor "chunks" between the plates. The modules are designed to have heat flow from the large area of the hot side ceramic plate to the cold side ceramic plate. Thus, from the hot side to the cold side in a circuit model for this element, there
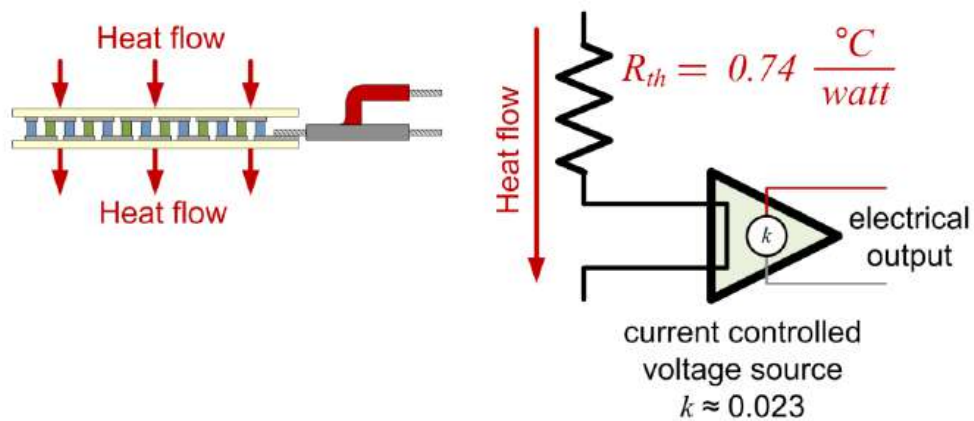

Figure 5.   Simplified model for TEG module.

will be a thermal resistance. From the manufacturer's specification, the thermal resistance is $\sim$0.74°C/W. The open circuit voltage generated by the module is $\sim$23.0 mV/W passing through the module, but will be a somewhat nonlinear function of the temperature difference across the module.

The model for this element is a mixed electrical and thermal circuit because it has a thermal input/output and an electrical output. The mixed thermal and electrical representation is no problem for the simulator – SPICE does not keep track of what is thermal and what is electrical (the user must keep track). A simple model for the TEG module is used for the Letts calorimeter because only its open circuit output voltage is measured (modulation of the thermal resistance by the electrical load is ignored). For this case, the module is represented as a thermal resistance and a current controlled voltage source as in Fig. 5.

3. Overview of the Letts Discharge Reactor and Calorimeter

The Letts gas discharge reactor (LENR Tube, LT) and its surrounding calorimeter are described in another paper [2], and is only briefly described here. The core reactor is a 28 cm long by 2.5 cm diameter coaxial stainless steel gas discharge vessel having a central molybdenum wire anode and an interior tube surface (cathode) electroplated with the active LENR metal (typically Pd, see Fig. 6). The tube is evacuated and then filled with $\sim$10 torr of D_2 or H_2 (for comparison). The power source for the discharge is a 200 mA constant current source which typically operates at about 330 V DC (66 W input) when the discharge has been struck. It was found that the desired pressure (10 torr) must be in place before the discharge is struck. Heat is taken from the system radially from the outside of the tube envelope.

Around the LT is a large copper block (photo in Fig. 3) with a large central bore for inserting the LT assembly; and eight small holes on a common radius for four inserted resistive heater cartridges ("HTR"), and four thermocouples ("TC"). The heater cartridges are used to raise the quiescent temperature of the copper block and LT. Calibrations of the system are normally taken with the resistive cartridge heaters set at a fixed power, or changed to keep the total input power constant (discharge power + resistive heater cartridge power).

The purpose of the large copper block is to thermally sum the heats coming from the LT and the resistive block heater cartridges, and distribute the heat to flow through the TEG modules into the finned aluminum air cooled heat sinks, with the heat flow registered as an output voltage on the TEG modules. The copper block, TEG modules, and aluminum heat sink comprise the core of the calorimeter. To help maintain repeatability, the calorimeter is housed in constant temperature commercial refrigerator with a set point temperature of 28°C.

Typical experimental protocol involves filling the LT with D_2, establishment of LT discharge, looking for excess heat (XH), and if XH is found, evacuate the LT and repeat with H_2 to show quenching of the XH – presuming and proving isotopic dependence of the XH effect.

Note that modeling the temperature of the aluminum heat sinks inside the temperature controlled chamber is unnecessary for some experiments when thermocouples are present to measure their temperatures. In the model, this can be represented by forcing the temperature of the heat sinks to be the experimentally recorded value, minimizing unknowns in the model.

4. Thermal Model Circuit Development

Thermal model circuits are generally much less complex than most electrical circuits because the model is comprised of such few element types: thermal sources, thermal resistances, and thermal capacitances (which are always to ground). The TEG modules are somewhat unique to the application, but are simple fundamental sub-circuits.

In development of a thermal circuit model it is desirable to recognize which heat flows can be combined into one element (or path). For example, consider the copper block at the heart of the Letts Calorimeter as shown in Fig. 7. The block and its coupling of heat is symmetric around the center to its four sides; I.E. heat is taken out of all four
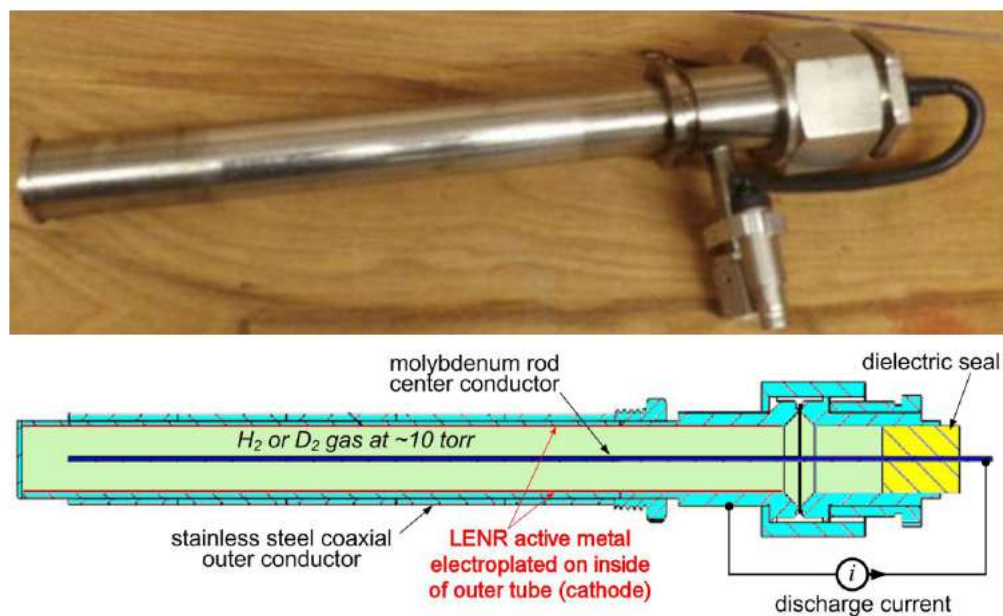
Figure 6.   Gas discharge "LENR Tube" (LT).

sides in the same way. Heat enters radially distributed around the block center from the outer shell of the LENR tube (LT). Provided the remainder of the system remains symmetric, all of the heat conduction path resistors are essentially parallel and may be modeled by just one equivalent combined thermal resistance. The intention is not to model the heat flow distribution on each side, since there are no measurements to support that modeling. The resistor flow paths on a single side can be condensed into a single flow path for the circuit model. All of the LT heat will come in at P_i and pass through a single combined/effective thermal resistance that will model the combination path to all four sides. This is a tremendous simplification of the model circuit – it means that only one value (R_{equiv}) will have to be found that provides a good match to the measured response.

Also, consider that each side of the copper block will have five TEG modules arranged along its length (see Fig. 8), through which the heat will flow. The module electrical outputs are wired in series. There is no need to put five modules in the model – put a single TEG model and presume all of the heat from the five TEG modules flow through the one module – the heat flow will be five times that going through the single module and the voltage output of the single effective model TEG module will be five times that of a single module. The same is true for each of the other module sides – these can again be combined into a single module representation with all of the heat from the 20 TEG modules flowing through a single equivalent module – a substantial simplification!

Only when it is found that this contraction of the model produces a circuit whose response cannot match that of the experimental device should one consider expanding the circuit into more of a 2-dimensional model. Try a simple circuit first – it is usually found that even a simple circuit model can represent a great deal of complexity in the output response.

Problems with matching the experimental and simulated responses are not always caused by the simplification into a single path model – sometimes other phenomena are present. High temperature difference and air flow convection and radiation mechanisms can combine to make the resistance non-linear – meaning that the resistance is smaller for
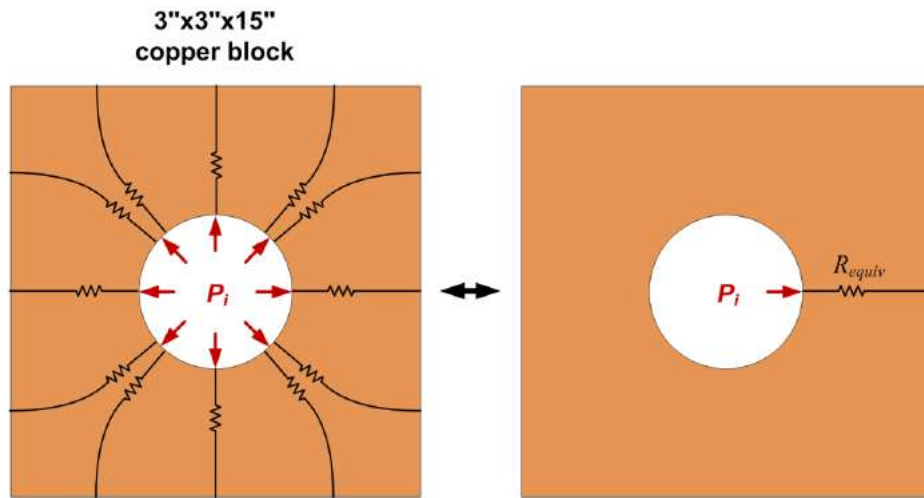
Figure 7. Thermal model for copper block.

a large temperature difference than it is for a small temperature difference. The fix for this problem is to use a single non-linear resistance rather than trying to find topology changes in the circuit. Note that the thermal resistance of a path within a metal is seldom non-linear over the temperature ranges likely to be modeled.

Try to maintain a direct 1:1 correspondence between your circuit and the physical structure. Another rule of thumb is to start simple and add additional heat paths as needed to achieve a match between the experimental response and the simulated response.
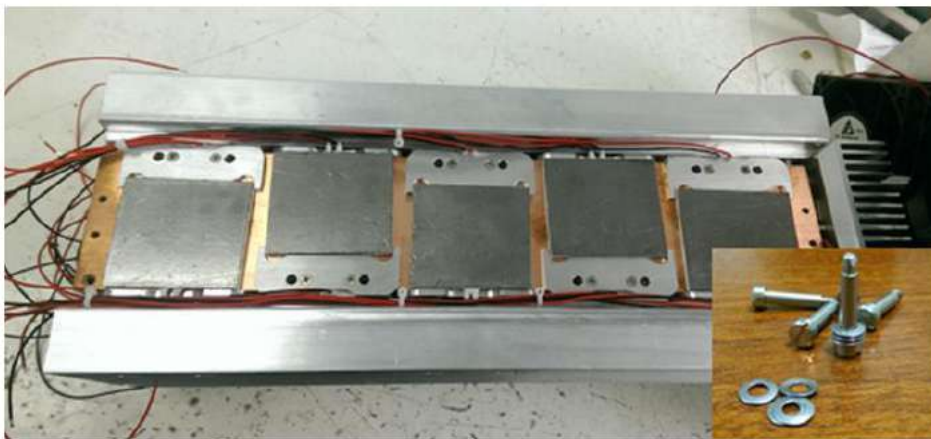
Figure 8. TEG modules along length of copper block.
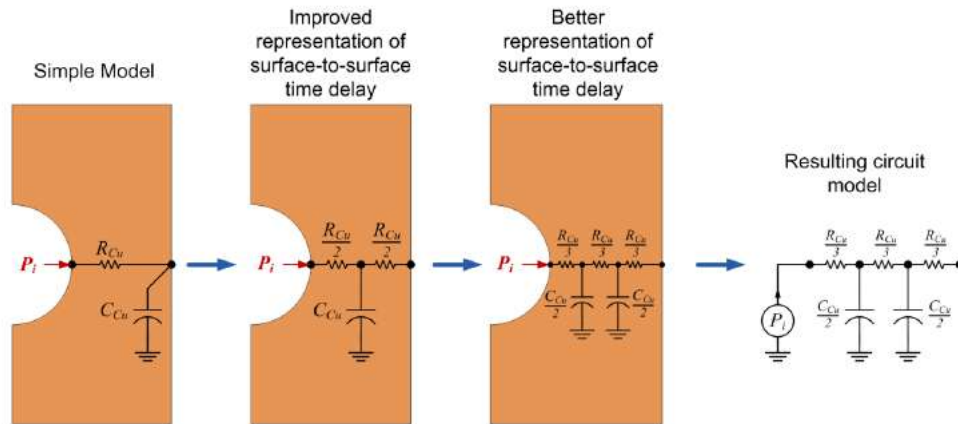
Figure 9. Dynamic thermal model for copper block.

4.1. Thermal model dynamics

The dynamic response of the model is primarily due to heat storage in thermal capacitances. The model of Fig. 7 of the copper block did not include the thermal capacitances that would have provided the dynamics of the heat flow. Generally, the dynamic response is sensitive to the $R-C$ product time constant, and much less sensitive to the absolute accuracy of either R or C.

The simple model for the copper block would be an $R-C$ as shown in Fig. 9 (circuit at the far left). However, the nature of the flow from the inner surface where the heat is applied from the LT to the outer surface of the block, where the heat is extracted through the TEG modules, is of a more distributed nature. Thus, an improved model comprises breaking the $R-C$ into multiple sub-sections – a more distributed $R-C$ delay wherein the total resistance and capacitance has not changed. Seldom is there an advantage to breaking the circuit into more than two capacitances and three thermal resistances.

Consider that the heat source is represented by a constant current source (current being the analogue of heat flow in watts).

4.2. Modeling the core copper block

Holes for the heater elements in the block and for the thermocouples are ignored – the absolute value of the thermal capacity is of less importance than the time constant of the system, which will be extracted from experimental data. Figure 10 shows the dimensions of the core copper block. Its volume is computed as 128.3 in.^{3} = 2102.9 cm^3. Copper's density is listed as 8.96 g/cm^3 – the total weight of the copper block is ~18.8 kg. In Section 2.2, the thermal capacity of copper was found to be 0.385 J/(g °C); thus, the thermal capacity for this copper block is 7254 J/°C. In the model for the copper block, this will translate to a circuit capacitance of 7254 F (but it is divided in the distributed $R-C$ modeling).

4.3. Copper block with TEG modules and finned heat sinks

Heat from the Cu block is expected to largely pass through the TEG modules to the finned Al heat sinks, and subsequently into the forced air flowing past the heat sinks (primary path, see Fig. 3). As heat flows through the TEG
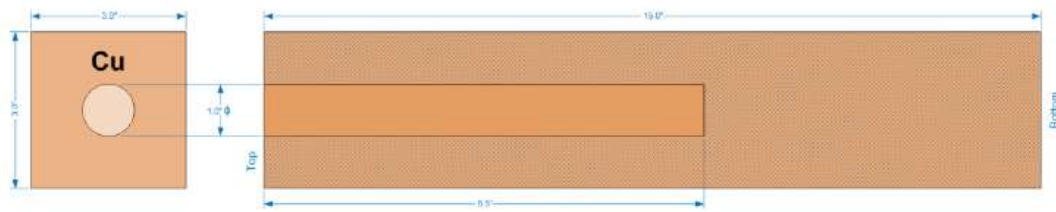
Figure 10. Copper block dimensions for mass calculation.

modules, the TEG voltage is recorded as a proxy of the heat flowing through the module. There will bea small heat leakage path from the Cu block directly to the ambient air that by passes measurement by the TEG.

Figure 11 shows the simple model for the Cu block assembly with its Al heat sinks. C_1 is the thermal capacitance calculated for the Cu block – it is partitioned into 2. Resistor $R1$ is partitioned into three pieces as part of the same distributed $R - C$ delay network. The primary heat conduction path is through thermal resistance, $R4$, for parallel combination

Of the thermal resistances of all 20 TEG modules. The per-module resistance was stated in Section 2.5, Fig. 4, to be 0.74°C/W. For 20 modules the thermal resistance is reduced by a factor of 20, so R4 in the model would be $(0.74/20) = 0.037 \ \Omega$ (a very small value!) The unknown for the TEG modules is the k_s thermoelectric conversion constant that will be determined by extraction so as to match test experimental data.

Thermal resistances R3 and R5 represent the heat leakage flows from the Cu block to ambient and to the Al heat sink, respectively. R3 and R5 are unknown and will be difficult to separately extract from the test data. Initially R5 will be ignored and all of the heat leakage will be lumped into R3.

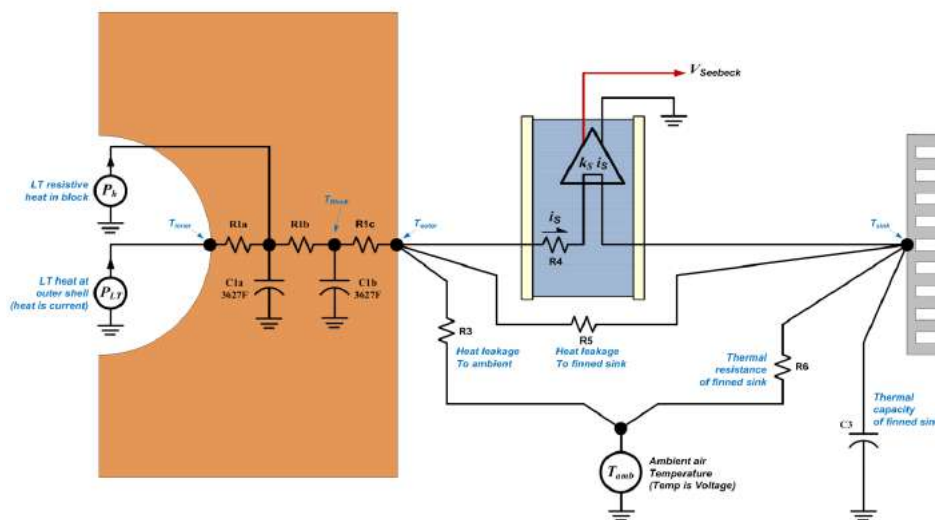An important simplification is shown in Fig. 12. Since the data acquisition records the heat sink temperature, the

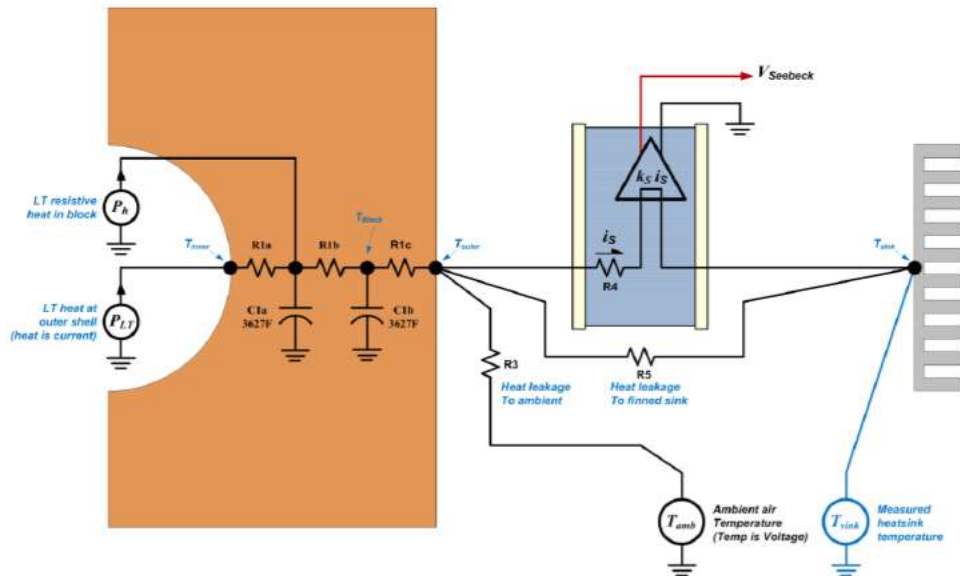**Figure 11.** Simple circuit model for Cu block, TEG, and heat sink assembly.

Figure 12. Reduced circuit model.

model can be driven with a voltage source (temperature) to constrain the circuit to have the experimental temperature for the heat sink. This will remove heat sink thermal behavior from the model – its state variable (its temperature) is known/forced as a function of time. Once the R1, R3 (ignore R5 for now), and k_s are determined, then R6 and C3 may be extracted by choosing values for them that cause the measured heat sink temperature to reproduce the experimental value of T_{sink} vs. time without a source driving the heat sink node.

"Parameter extraction" is determination of the model circuit values by iterating the unknown model circuit values to cause the simulated output(s) to match the measured experimental output(s). A first estimate is made for the model element values and the simulator is run with the known/measured values for the input waveform(s), and provides simulated output waveform(s). The simulated output waveform(s) are compared to the measured/experimental output waveforms, and the model element values are adjusted to bring the simulated output(s) to closer to the measured waveform(s). This process is repeated until sufficient agreement is reached (Fig. 13). When agreement is reached, the model parameter values are said to have been "extracted" – this is the objective.

Once the parameters have been extracted, the model is ready for use. Referring to Fig. 14, if the simulator is driven with known input waveforms (and 0 for XH), then the simulated outputs will match the experimentally measured null experiment output waveform(s). I.E. the model will represent the known/expected response from the known inputs.

Suppose a new experiment is run, this time with an unknown LENR XH being generated sometime during the experiment. For this experiment, the model can take the known/measured power inputs and provide the expected output corresponding to those inputs if there is no XH. The modeled output may be used to extract the waveform for XH – but it is not a simple problem. In general, this problem is a class of deconvolution, which is well known to be an "ill-conditioned problem". It is ill-conditioned because of noise in the measured data. If the system comprises a delay (typical), it will exhibit a low pass response – the XH high frequencies will be attenuated in the measured output and the signal-to-noise ratio (SNR) for the high frequencies of the waveform will decline continuously as the frequency
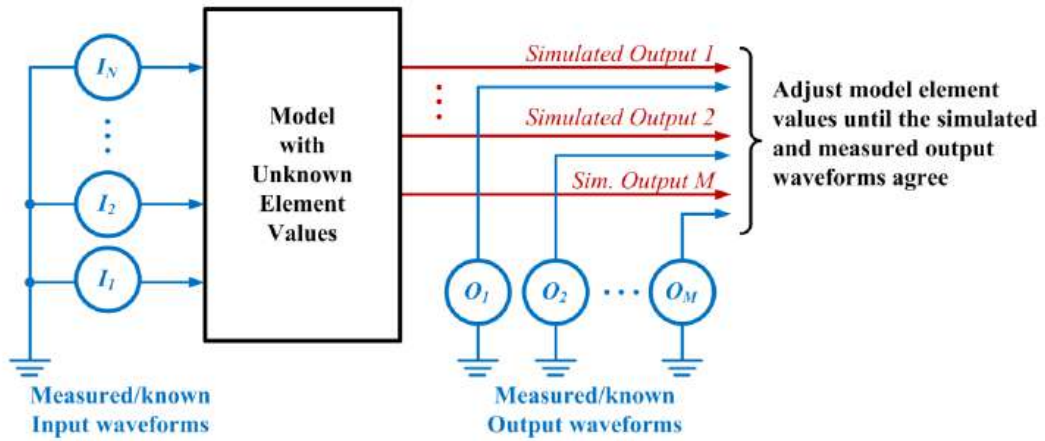
Figure 13.   Model parameter extraction.

increases. At some frequency within the unknown XH waveform, the response in the output data will just be noise. Reconstruction of the high frequency components of the XH from the noisy output waveform will, by virtue of the noise, become arbitrary. Thus, one must limit the reconstruction of the XH (in extraction) to a component frequency range having real supporting data (SNR) in the output waveform. The better the output can be measured (lowest possible noise), the better the XH waveform can be extracted/reconstructed.

Because the system is likely to be non-linear, deconvolution cannot be done by Fourier techniques. Generally the solution requires iteration – take a guess at the XH waveform, find the output (experimental- simulated) difference, and construct a better guess at the XH utilizing the difference. Repeat this process until the simulation using the XH
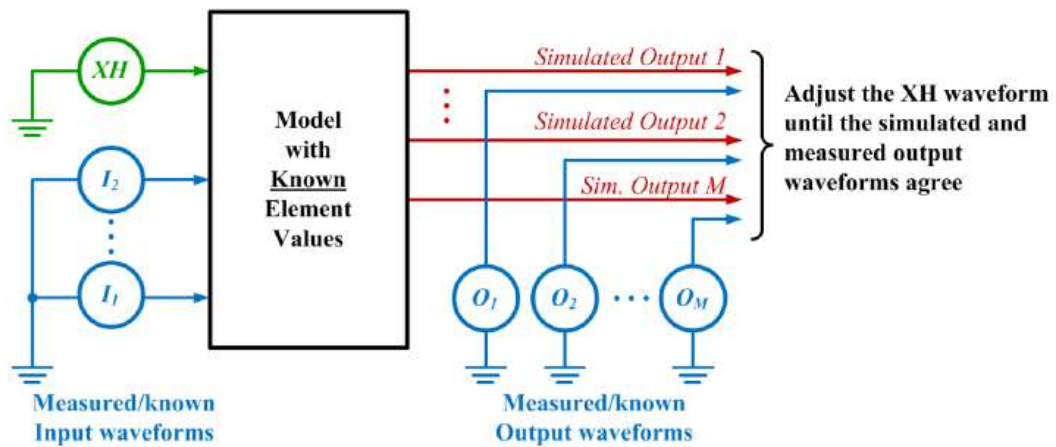
Figure 14.   XH extraction.
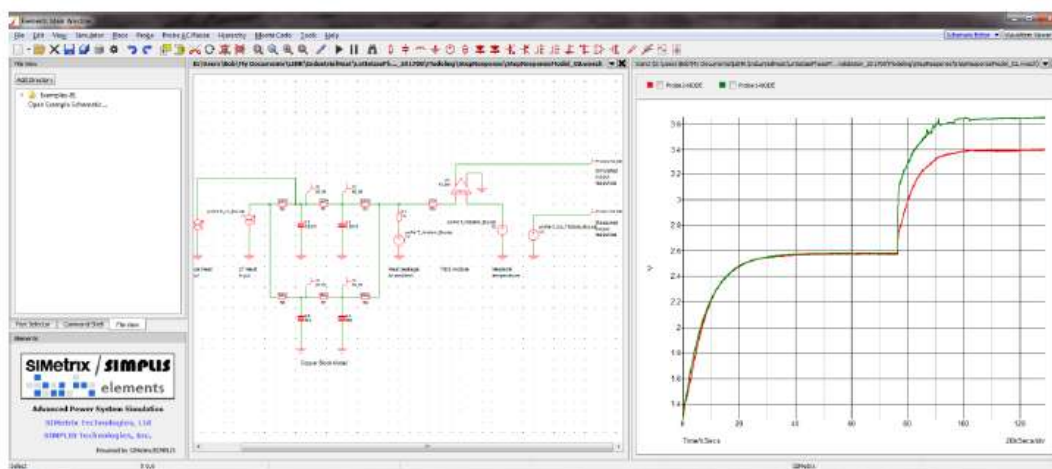
Figure 15. Step response of calorimeter.

waveform creates a simulated vs. experimental output difference of essentially zero. With this process, the XH versus time waveform may be extracted.

Fortunately, an easier way to perform this extraction using the power of the simulator exists, and will be described below.

5. Modeling With The SIMetrix SPICE Simulator

A description of how to use the SIMetrix SPICE simulator is deferred to its well developed manuals. Figure 15 shows a model entered into the SIMetrix SPICE schematic editor. The circuit is easily entered with the graphical interface, and graphical outputs are managed in another window (windows are un-dock-able). Any of the currents/powers and voltages/temperatures may be probed after the simulation has completed by selecting a probe type, and clicking on the desired branch/node in the schematic.

Early on, an experimental run was created with a canonical step heat input waveform. The step input excites the natural response of the system. A curious effect was noted in the experimental data (see Fig. 16). In this figure, the blue curve is the actual step heat input into the calorimeter (non-ideal). The red curve is the heat proxy measured by the calorimeter via the TEG voltage output (approximately calibrated to translate to power measured). What is seen is that more than one time constant is present. The output initially rises quickly, with approximately 40% of the heat registered in a very short time. Following the initial rise, the remainder of the heat is registered in the output with a longer time constant as expected (∼119 min). Close examination (see Fig. 17 zoom) showed the faster time constant to be ∼2.7 min – 44 × faster! The initial rise is so fast that it is poorly sampled by the 1 min sample period of the data. While the initial rise is fast compared to the main propagation of the heat through the block, it is still slow compared to a "speed of sound" effect. As the model development progressed, it became clear that this second propagation mode was real, repeatable, and present in the response at all excitation levels.

The plots were sent to the manufacturer of the TEG modules who suggested that the response could be due to non-linearity in the power flow to voltage output conversion. A university professor suggested that the response appeared to be a "non-Fourier" heat transfer mode – poorly documented in the literature [3]. The existence of the second mode, as opposed to a non-linear response, was confirmed by excitation with a stair-step power waveform in place of the
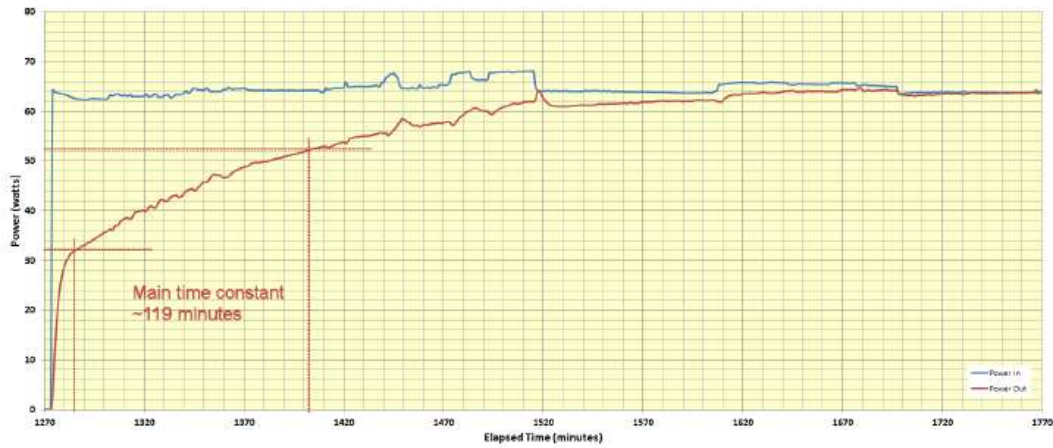
Figure 16. Step response of calorimeter at TEG output.

single large step (see Fig. 18). Each of the individual small steps showed the dual time constant which would not have occurred if the response shape were due to non-linearity in the TEG. While this anomalous, non-Fourier heat flow mode is interesting, it is simply noted here that there is more than one heat propagation mode in the system. The second propagation mode just adds additional complexity to the model.

Data from a calibration run having stepped electrical power applied to the resistive heaters in the copper block (LT still present, but no discharge current supplied) was used in model development. The resistive heaters were driven in a stair-step (DC) in power steps of 20 W from 0 to 200 W (Fig. 18).

Figure 19 shows an early single propagation mode model for the calorimeter (after the benefit of iterative parameter adjustment). On the left, I2 is the heat input versus time as a PWL current source playing out the measured data for the
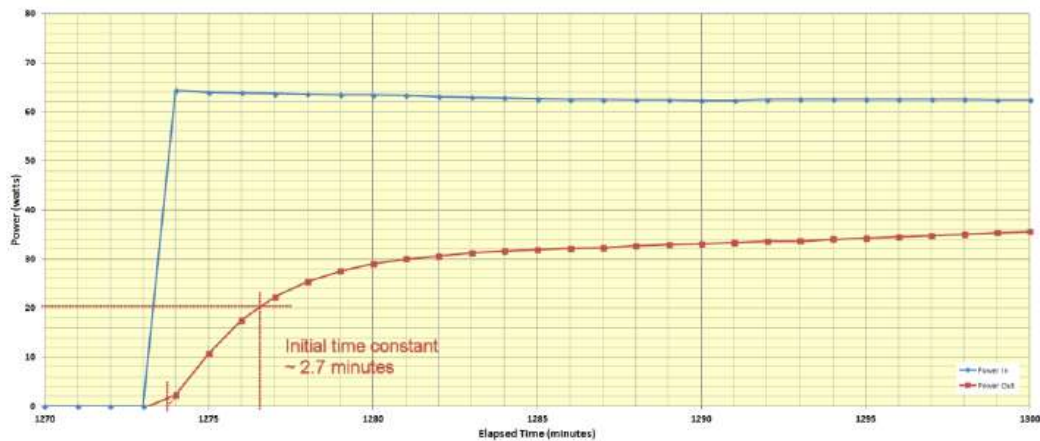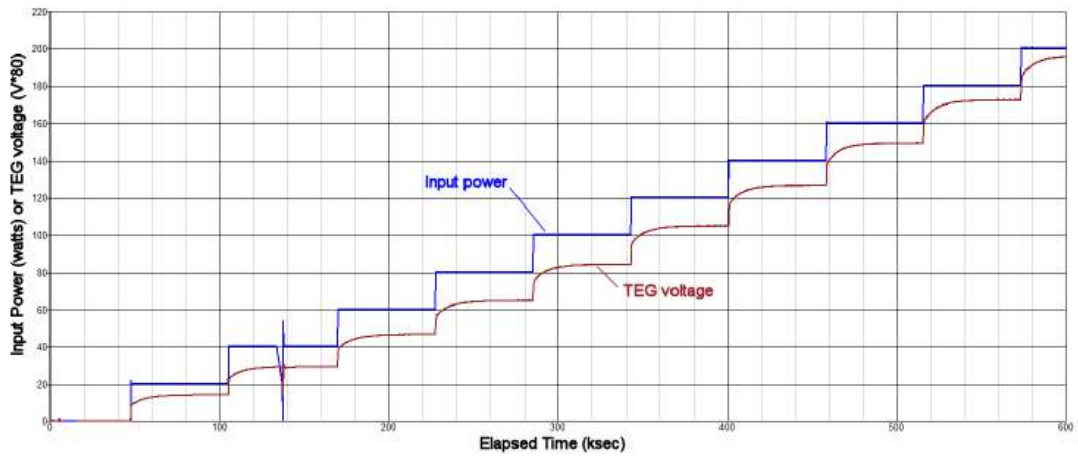

Figure 17. Anomalous fast rise.

Figure 18. Stair-step excitation and experimental response.

input heater power. V1 is the ambient temperature versus time; and V2 is the block's heat sink temperature versus time (being driven by the measured data). V3 is simply playing out the measured TEG output voltage for graphing. Around these sources is the model for the block and its TEGs. The output voltage from the TEGs was found to be non-linear, and a non-linear transfer function block (ARB1) was included in the TEG model. The small symbols labeled "IC" stand for "Initial Condition". These provide the simulator with starting conditions ($t = 0$) for the state variable – in this case the temperature of the node. The IC is placed as a component in the schematic, but it is actually a simulator directive.

Figure 20 shows the simulated TEG output voltage in response to the experimental input power at I2 and compares it with the experimental TEG voltage supplied at V3 (for convenient graphing only). The response shows a good match at the settled points for the 0–200 W stepped input power.

However, one can see the difference in the step response dynamics between the single mode simple model and the
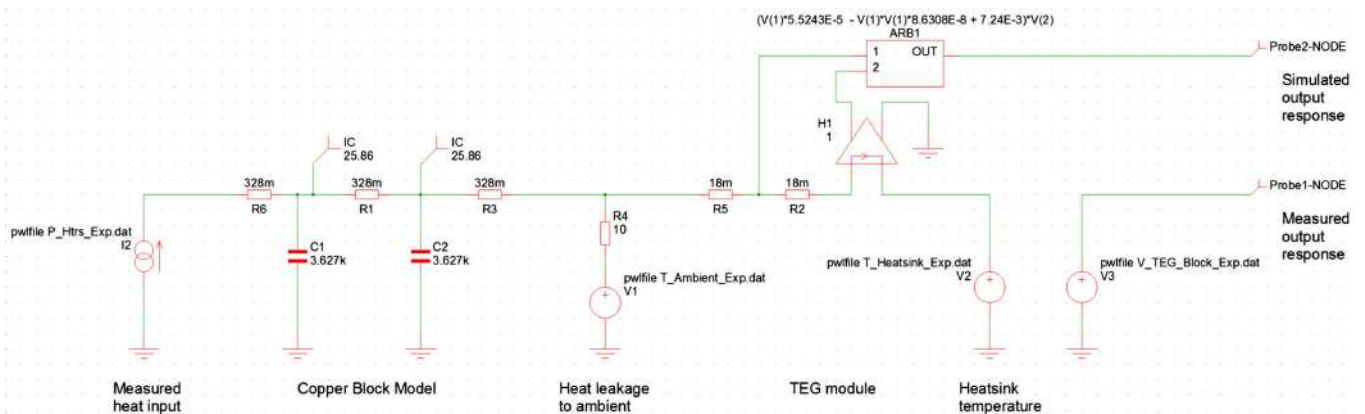

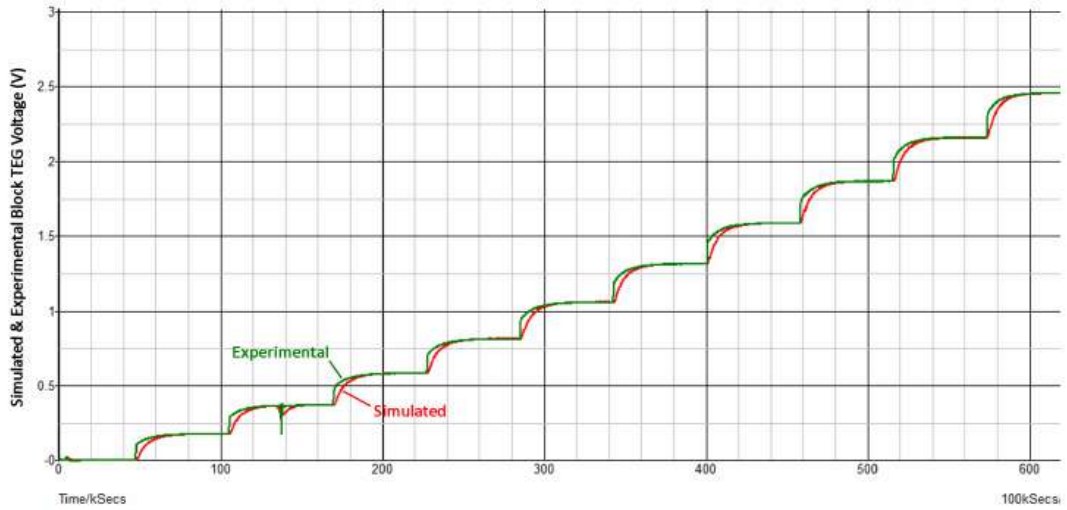**Figure 19.** First pass single heat flow mode model.

Figure 20. Response of first pass single mode model.

actual behavior of the real experimental copper block – the experimental data rises much faster initially at each step due to the previously described second mode.

This fast early rise can be clearly seen in the zoom of one of the steps in Fig. 21. To achieve a good match between simulation and experiment, a second delay/propagation mode must be included in the model.

Including a second propagation mode in the model began with a parallel $R - C$ track in the model for the copper
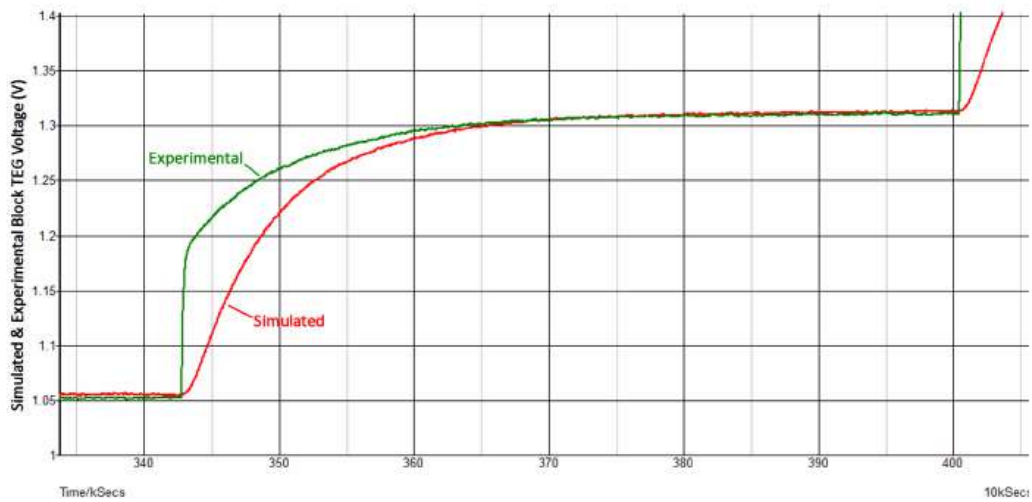
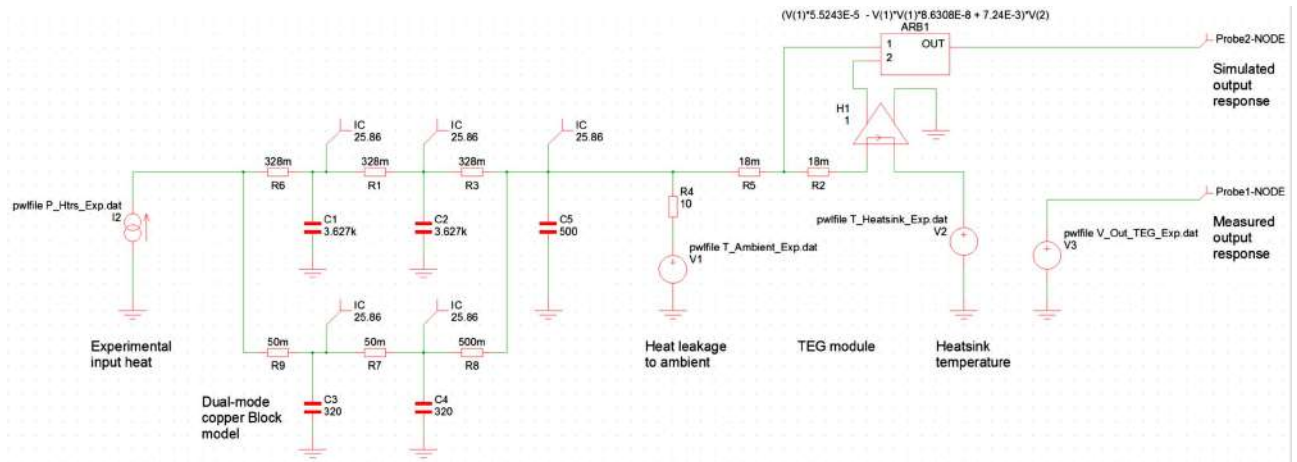**Figure 21.** Response of first pass single mode model (zoom).

Figure 22.   Second pass dual mode model.

block. Figure 22 shows a second schematic having the parallel $R - C$ tracks. When Fig. 22 was simulated, it clearly showed both the fast and the ordinary modes. The amount of the input delivered into each mode was determined by the size of R9/R7/R8 compared to R6/R1/R3. Adjustment of the values proceeded to provide a better match of the output dynamics near the beginning of the steps, but it was found there were not enough element values to change to provide a smooth transition from one mode to the other as was actually seen in the experimental response.

While the dual $R - C$ delay path model shown in Fig. 22 provided a visualization of the transition from a single-mode model to a dual-mode model, the topology did not provide a good match for the dynamics of the steps. Figure 22 circuit model was abandoned in favor of a new heuristically derived topology (Fig. 23) that would provide a better match for the response at the expense of having lesser visualization of the presence of the two modes. Figure 24 shows the good match between the experimental and the modeled response to the stair-step power input. Note that the glitch in the stair-step input at ∼139 ks was a power failure that was recovered. Using the actual measured input data to drive the model (using a PWL source) insures that this event is included in the input. Figure 25 is a zoom at a step in the
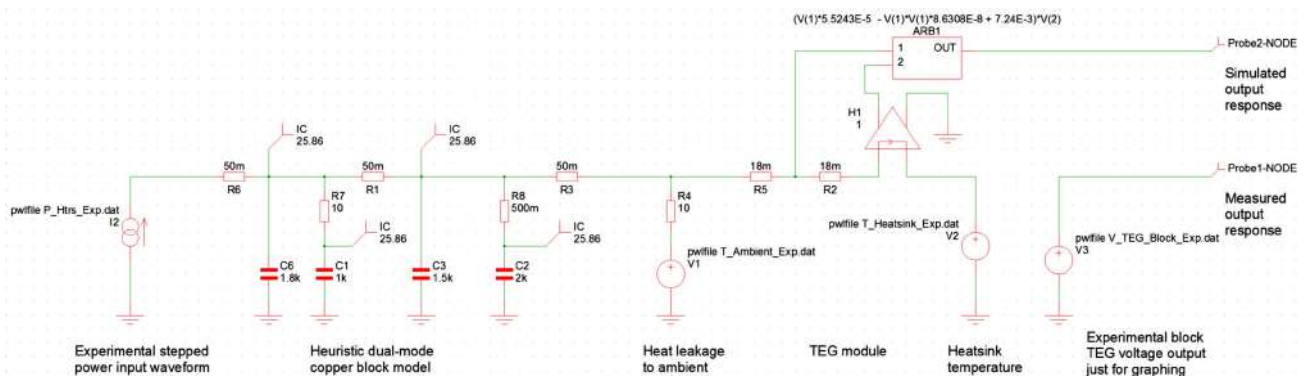

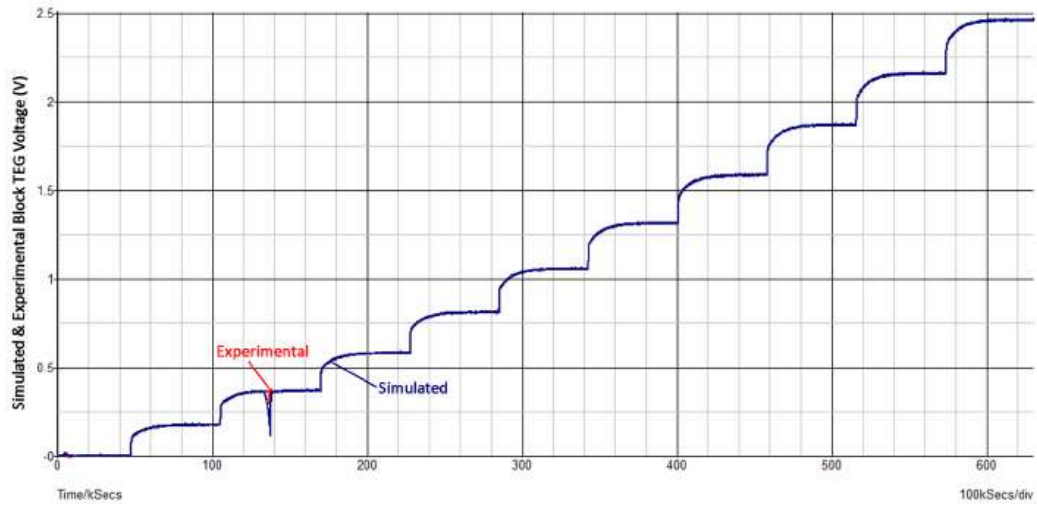**Figure 23.**   Third pass heuristically derived model.

Figure 24. Stair-step response of third pass model.

power input, showing the match to the dual mode dynamics.

Up to this point, it was presumed that all of the input heat was going into the copper block for simplicity. Only ∼5% of the heat exits the calorimeter through the "Lid" – the top cover of the calorimeter having its own TEG modules. The fourth pass of the model addresses the addition of the Lid.

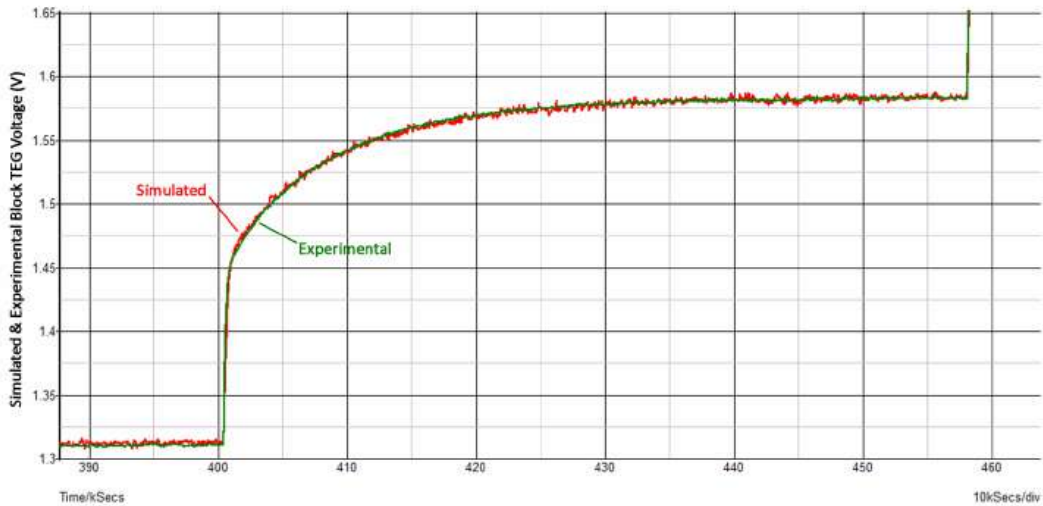To include the Lid in the model, circuitry was added to divide the incoming heat between the block section and the

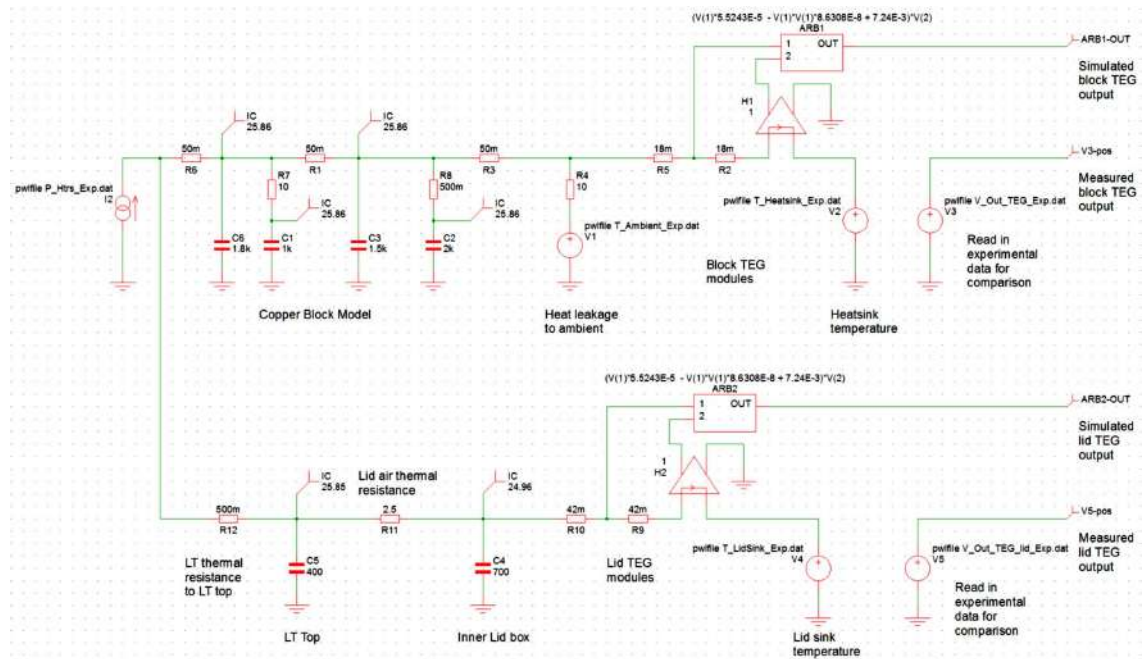**Figure 25.** Response of third pass model to stair step (zoom).

Figure 26. Schematic of the fourth pass model including the Lid.

Lid sub-model. A second output was created from the Lid TEG module(s). Heat is delivered to the Lid by conduction from the bottom portion, radiation from the LT top, and convection through the air in the Lid. Figure 26 shows the fourth pass model having elements to model both the block and Lid. The model for the block section has been adjusted slightly to account for the heat coupled into the Lid. The TEG modules were modeled the same for the Lid, but the thermal resistance was changed due to fewer modules. Non-linear resistances were used to model the heat flow in the air in the Lid to better fit the experimental data.

Figure 27 shows the excellent fit of the simulation to the block TEG voltages in the fourth pass model over the entire 200 W stepped range.

5.1. Extracting the XH wave form

The goal of this modeling effort is to provide a means to extract, in a calibrated way, the XH occurring within the Letts calorimeter. Once the model has been extracted, determination of the XH waveform is a problem in deconvolution, as mentioned in Section 4.3. Fortunately a solution has been found to use the power of the simulator to perform this deconvolution with no manual iteration. The technique also has promise for single parameter extraction in model development.

Consider the hierarchical schematic in Fig. 28. The extracted model for the LT and calorimeter are packed into the "Seebeck SubModel" block with its inputs provided at the left and the outputs (block and Lid TEG voltages) on the right. The ARB1 block in the figure simply combines (sums) the block and Lid TEG voltages and subtracts the sum of the experimental block and Lid voltages – producing a difference at each instant in simulation time of the simulated and experimental responses.
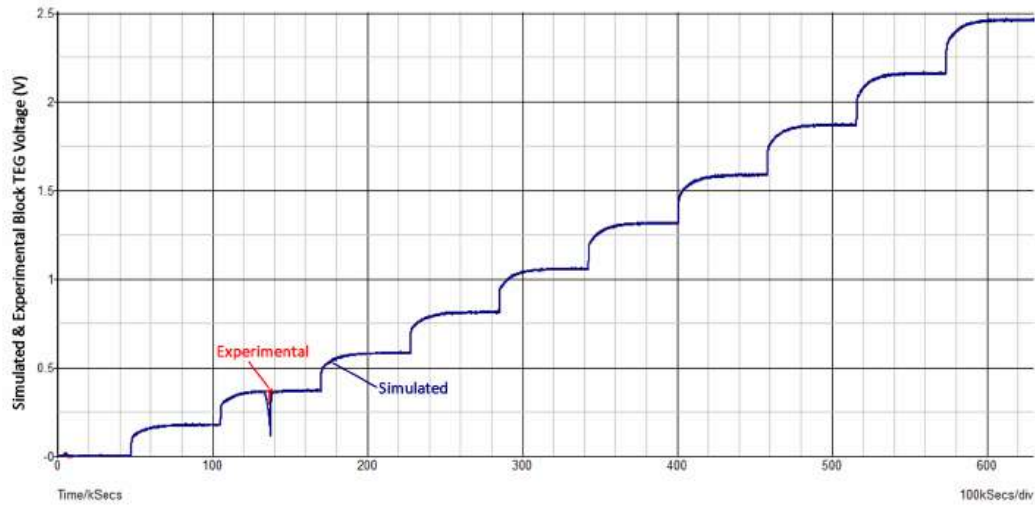
Figure 27. Fourth pass model block TEG response.

The high gain amplifier G1 (voltage in, current out) provides a negative feedback to the heat input node (left side of the SubModel block), attempting to force the difference between the simulated and experimental results to zero. If there is no difference between the modeled and experimental heats (a null experiment), then G1 will supply no feedback correction. If there is an XH , the experiment will have more output power than the model, and G1 will supply (via negative feedback) the heat necessary to balance the model output with the measured output. The XH waveform would be the feedback current.

To test whether this circuit can extract an XH waveform, source I1 (an ideal waveform generator) is placed in the model as an injected XH waveform in an otherwise null experiment. If I1 is zero, no XH is detected in the feedback current. Figure 29 shows the feedback current XH extraction when the I1 waveform is a triangle wave of mock XH
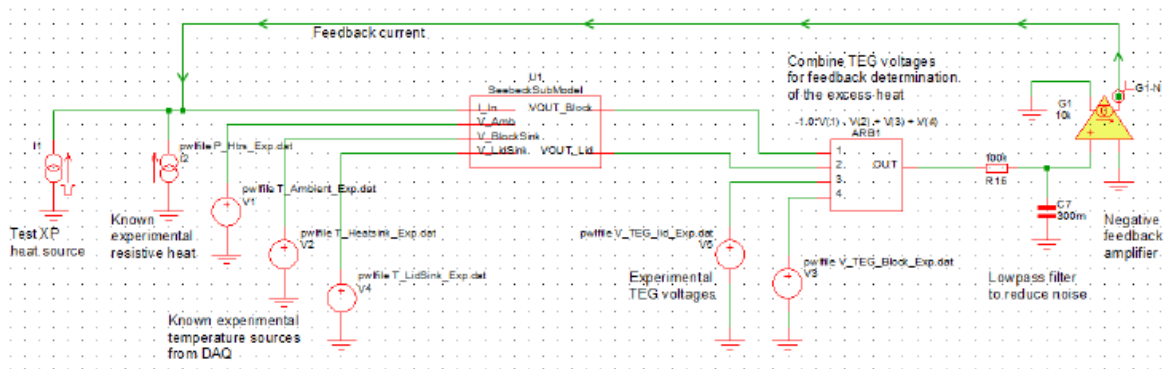

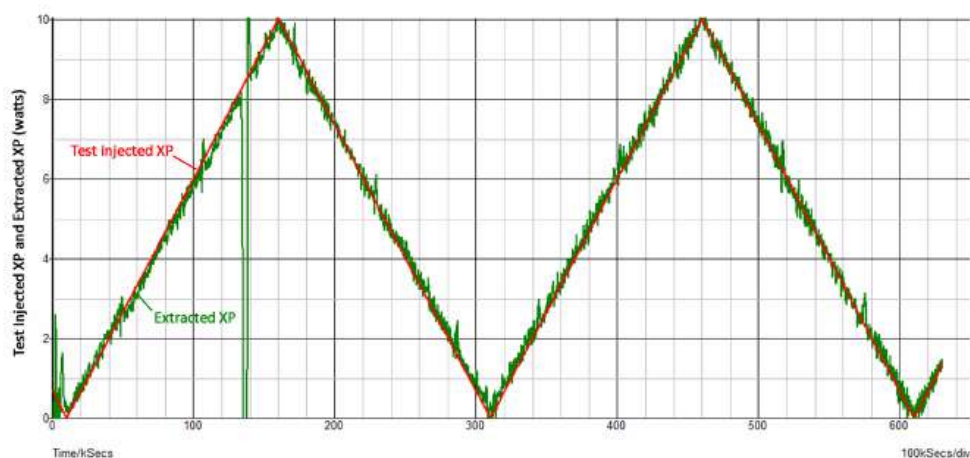**Figure 28.** Feedback solution for XH.

Figure 29. Feedback extraction of mock XH waveform.

power. While there is noise in the feedback waveform (expected), the feedback does a good job of reconstructing the mock XH that was injected.

Note the low pass filter between the ARB1 block and the G1 amplifier. This limits the bandwidth of the feedback signal and hence the representation of the XH waveform. A lower bandwidth of this low pass section will reduce the noise, while increasing the feedback gain at G1 increases the noise. For each system, a trade-off will have to be made between feedback gain at G1 which reduces the error in the waveform, and the low pass bandwidth that reduces the noise and the high frequency components of the extracted XH waveform. Since this extraction used driving data from a null experiment, some of the noise is quantization noise from the coarsely sampled measured data that is linearly interpolated by the simulator. Sampling at a smaller period would reduce this noise.

As further verification, a null LT was created having a resistive heater in place of the discharge in the tube. As a simulation experiment, the heat to this null LT heater was driven with a stepped waveform and the model was tested in its ability to recover the heat that had been applied – the results are shown in Fig. 30. As can be seen, the input waveform comprised very high bandwidth steps, and aside from the ringing produced by feedback around the low pass response (common in deconvolution), the technique faithfully recovers the resistive LT heater waveform.

6. Additional Modeling Considerations

As modeling of actual experiments was attempted, a number of other factors affecting the response were noted:

- It was discovered that the wires leading to the heater cartridges were not copper for the full length up to the inserted cartridge – there was in one case up to 1 m of nickel wire. Heat generated in the resistive loss of this wire was not deposited into the copper block, but it was measured as part of the input heat. This effect can be included in the model, but it would be better to make a measurement of the heater voltage with 0-current wires tapped onto the heater cartridge as it enters the copper block (a 4-wire connection).
- Un-modeled heater lead wire resistance will lead to calibration scale error.
- A heat storage effect was found inside the discharge tube (LT) itself. While there may only be 10 torr of gas inside the tube, it is heated to an effective temperature of $\sim 2500°C$ when the discharge current is turned ON.

This heating not only has a rise time, but the heat is released when the discharge is turned OFF. This can be modeled.

- There is a small heat removed when the gas is evacuated from the LT. If evacuation occurs even minutes after the discharge is stopped, there is little heat lost to the system in evacuation. However, when the evacuated tube is re-loaded with gas, heat may be removed due to injection of cool gas, or Joule–Thomson gas expansion may add or removing heat from the system (J–T expansion is generally a cooling effect except for H_2, He, or Ne). This effect could be added to the model.
- Discharge current flowing when the gas pressure is less than about 2 torr in the Letts LT geometry causes two problems. The glow forms closer to the top of the LT and disproportionally heats top and Lid of the calorimeter. Second, the thermal conductivity of the gas declines and the center conductor of the LT can get hot causing thermal conduction to the top of the LT. Thermal imaging during discharge with the tube outside the calorimeter is a good diagnostic to determine the safe operating region where heat will be deposited along the length of the LT.

7. Experimental Versus Model-extracted XH

Letts experiment 780 is provided as an example of the difference between XH ("Directly extracted XP" in Fig. 31) calculated using the simple differential calibration, and the XH extracted using the model ("residual" in Fig. 31).In the figure, the simulation extracted XH is labeled "residual" because it is that which remains in the feedback power (current) when all known heat sources have been accounted – it is presumed to be LENR heat. The experimental protocol is complex due to attempts to find the triggers of the XH , and to quench the excess by substitution of light hydrogen for deuterium.

With the aid of the model, simulation extracts the true behavior of the XH flow in this experiment. The extracted XH proves to be lower in magnitude than that found from simple differential calibration. The excess power waveform (the residual) shows fewer endothermic regions and of smaller magnitude. Many of these endothermic excursions are caused by evacuation and gas change in the LT during the experiment; the Joule–Thomson thermodynamics of which
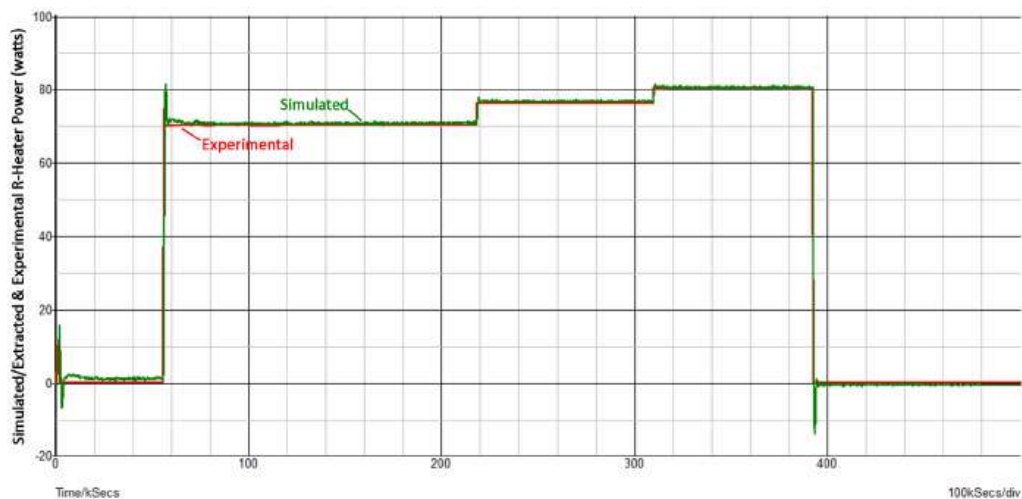
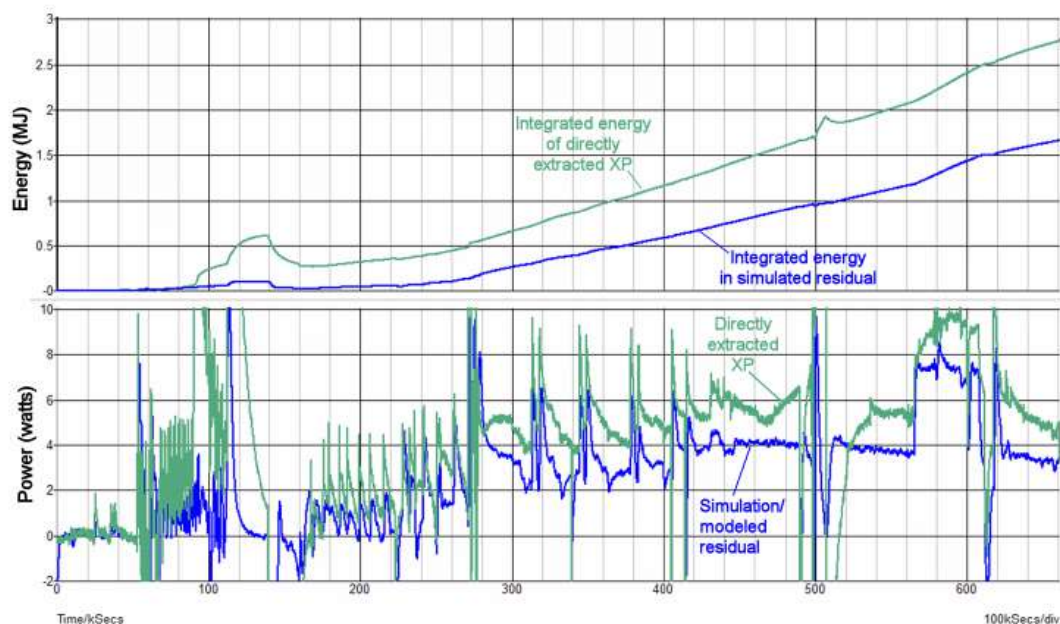**Figure 30.** Simulation extracted null LT heater waveform.

Figure 31.   Experiment 780 XH .

are not entirely captured in the present model. Notice that when excess power is present in the simulation extracted residual, the excess power turns ON quickly, and is much flatter than what is found from the excess power taken directly from the differential calibration. This is because the simulation de-embeds the long thermal dynamics of the copper block in the calorimeter from the response waveform.

8. Conclusion

A technique is presented showing how electrical circuit analogues may be used to model a complicated thermal system. The SPICE simulator may be used in transient simulation mode to evaluate the modeled response. Use of the SIMetrix SPICE simulation environment is convenient, easy to use, and free for simulation of small size problems. The electrical circuit analogue technique for thermal modeling requires some effort to extract a topology and component values to provide a good fit to the response of the apparatus, but the resulting simulation is highly efficient – almost always requiring less than 5 s of computation on an ordinary 2018 personal computer. During the course of model development, substantial understanding of the measurement system and its limitations will be developed that may be missed if only differential calibration is utilized and new sources of possible error and inaccuracy may be overturned. Additionally, opportunities for system improvement become obvious during the modeling.

   Model extraction using purpose run null experiments improves the quality and accuracy of the extracted excess power (residual) compared to use of a single calibration run and differential calibration for residual extraction. Essentially the modeling incorporates information from the calibration runs which is all ultimately brought to bear in computing the actual XH .

   An interesting thermal propagation mode was found in the copper block – possibly a rarely documented non-Fourier heat transfer mode. The TEG modules, as thermal flow sensors, have a very fast response and are capable

of detecting such fast thermal propagation modes. It is noted that F. Piantelli implicates such a non-Fourier thermal propagation mode in the stimulation of LENR in his nickel rod experiments [4,5].

Acknowledgements

References

[1] SIMetrix/SIMPLIS Elements Simulator, Available for free from SIMetrix Technologies at: www.simetrix.co.uk/downloads/download-elements.html.

[2] D.G Letts and D.J. Cravens, Building and testing a high temperature Seebeck calorimeter, *J. Condensed Matter Nucl. Sci.* ICCF-21 (2018).

[3] N.I. Kobasko and SH. E. Guseynov, An explanation of the nature of thermal waves "a poker effect" on the basis of hyperbolic heat conductivity equation analysis and existence of free electrons in metals, *Recent Researches in Circuits and Systems* (2014), ISBN 978-1-61804-108-1, WSEAS Press, pp. 167–172.

[4] S. Focardi, V. Gabbani, V. Montalbano, F. Piantelli and S. Veronesi, Large excess heat production in Ni–H systems, *IL Nuvo Cimento* **A 111** (11) (1998) 1233–1242.

[5] F. Piantelli, Private conversation with Piantelli, 2016.

[6] M. Marz and P. Nance, Thermal modeling of power-electronic systems, *Infineon Technologies Application note*, available at: https://pdfs.semanticscholar.org/438f/69381bbdaf56d853f082e17c8d3c51a0ef6e.pdf.

[7] F. Christiaens and E. Beyne, Transient thermal modeling and characterization of a hybrid component, *Proc. Elec. Components and Tech. Conf.* IEEE 46 (1996), DOI 10.1109/ECTC.1996.517388.